Questions and Answers

Chapter 5

Questions

(Q1) *Why are normalized the feature vectors? In the normalization of the sample feature vectors, the mean and standard deviation extracted from the training set are used. Explain why.*

(Q2) *Infer the gradient descent flow of the surface S associated with the kNN region-based energy functional*

$$E_{region}(t) = \int_{\Omega_{in}(t)} k_{in}(\mathbf{x};t)\, d\mathbf{x} + \int_{\Omega_{out}(t)} k_{out}(\mathbf{x};t)\, d\mathbf{x} \tag{1}$$

(Q3) *Explain the influence of each of the terms involved in the evolution of the surface driven by*

$$\frac{\partial S(\mathbf{x};t)}{\partial t} = \zeta(k_{out} - k_{in})\vec{n} - \eta(g\kappa + \langle \nabla g, \vec{n} \rangle)\vec{n} \tag{2}$$

(Q4) *How could we determine the convergence of the level set algorithm?*

(Q5) *Explain what could be the advantages of using 3D models for quantification against 2D MIP images. Regarding the evaluation study presented in this chapter, was it taking real profit of the 3D measurement capability?*

Answers

(A1) The components of the vector of features vary from very different ranges. For example, the intensity values vary from 900 to 2500 whereas the absolute value of the eigenvalues usually is not bigger than 100. If the feature vectors are not normalized, the differences of the components with the biggest values can dominate in the calculus of the distance producing misclassification in the kNN rule.

Regarding the second question, the training set is chosen to explain the whole variability of patterns present in the images. So, if the set is significative enough, the values of the mean and the standard deviation are not supposed to differ too much from the ones computed from the whole sample.

(A2) Let be $\phi(\mathbf{x};t)$ a Lipschitz function such that

$$\begin{aligned} S(t) &= \{\mathbf{x} \in \mathbb{R}^3 | \phi(\mathbf{x};t) = 0\} \\ \Omega_{in}(t) &= \{\mathbf{x} \in \mathbb{R}^3 | \phi(\mathbf{x};t) < 0\} \\ \Omega_{out}(t) &= \{\mathbf{x} \in \mathbb{R}^3 | \phi(\mathbf{x};t) > 0\} \end{aligned} \tag{3}$$

Let be H, the Heaviside function, that is, $H(z) = 0$ if $z \leq 0$ and $H(z) = 1$ else. With this notation, Equation 1 can be written as

$$E_{region}(t) = \int_{\mathbb{R}^3} k_{in}(\mathbf{x};t)[1 - H(\phi(\mathbf{x};t))]\, d\mathbf{x} + \int_{\mathbb{R}^3} k_{out}(\mathbf{x};t) H(\phi(\mathbf{x};t))\, d\mathbf{x} \tag{4}$$

The first step is to compute the Euler Lagrange equation associated to the energy functional, by deriving it with respect to t

$$\begin{aligned} \frac{dE_{region}(t)}{dt} = & \int_{\mathbb{R}^3} k_{in}(\mathbf{x};t) \left[-\frac{dH(\phi(\mathbf{x};t))}{dt} \right] d\mathbf{x} \\ & + \int_{\mathbb{R}^3} \frac{\partial k_{in}(\mathbf{x};t)}{\partial t} [1 - H(\phi(\mathbf{x};t))]\, d\mathbf{x} \\ & + \int_{\mathbb{R}^3} k_{out}(\mathbf{x};t) \frac{dH(\phi(\mathbf{x};t))}{dt}\, d\mathbf{x} \\ & + \int_{\mathbb{R}^3} \frac{\partial k_{out}(\mathbf{x};t)}{\partial t} H(\phi(\mathbf{x};t))\, d\mathbf{x} \end{aligned} \tag{5}$$

As the variation of the kNN region descriptor in time is zero (the PDFs are time independent), and as $dH(\phi(\mathbf{x};t)) = \phi_t \delta(\phi(\mathbf{x};t))dt$, with δ

the Dirac's delta function,

$$\frac{dE_{region}(t)}{dt} = \int_{\mathbb{R}^3} [k_{out}(\mathbf{x};t) - k_{in}(\mathbf{x};t)]\phi_t\, \delta(\phi(\mathbf{x};t))\, d\mathbf{x} \tag{6}$$

As $|\nabla_\phi|\delta(\phi(\mathbf{x};t)) = dS$,

$$\frac{dE_{region}(t)}{dt} = \int_{s^{-1}(\mathbb{R}^3)} [k_{out}(\mathbf{x};t) - k_{in}(\mathbf{x};t)]\frac{\phi_t}{|\nabla_\phi|}\, dS \tag{7}$$

The minimum of the energy functional is reached when $\frac{dE_{region}(t)}{dt} = 0$. To hold this, the following condition is needed[1]

$$[k_{out}(\mathbf{x};t) - k_{in}(\mathbf{x};t)]\overrightarrow{n} = 0 \tag{8}$$

This is the Euler-Lagrange equation associated to the Energy Functional $E_{region}(t)$. So, the gradient descent flow associated to this equation is

$$S_t = [k_{out}(\mathbf{x};t) - k_{in}(\mathbf{x};t)]\overrightarrow{n} \tag{9}$$

(A3) **Region based term**: $S_t = (k_{out} - k_{in})\overrightarrow{n}$ with associated level set equation $\phi_t + (k_{out} - k_{in})|\nabla_\phi| = 0$.

The region based term acts like a balloon force maximizing or minimizing the volume inside $S(t)$ depending on the sign of $k_{out} - k_{in}$. Inside the object, the values of the region descriptor k_{in} are supposed to be smaller than the values of the outer descriptor, as P_{in} inside of the object to be segmented is high. For this reason, if the surface evolves inside the object of interest, as $k_{out} - k_{in} \geq 0$, the evolution proceeds outwards trying to maximize the volume inside $S(t)$. On the other hand, if the surface evolves outside the object of interest, the surface shrinks trying to capture inside only the points with high P_{in} with the purpose of minimizing the region-based energy functional.

Curvature based term: $S_t = -gk\overrightarrow{n}$ with associated level set equation $\phi_t = gk|\nabla_\phi|$.

A surface evolving under mean curvature motion shrinks while smooths down its boundary. As the curvature based term is multiplied by g, in places with flat gradient, the effect of shrinkage and smoothing is higher than in places with high gradient.

[1] The normal vector to the surface S can be computed from function ϕ as $\frac{\phi t}{|\nabla\phi|}$.

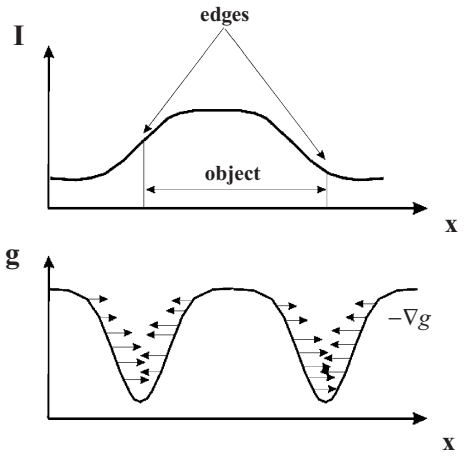

Figure 1: ID slice with the influence of the advection term in the edges of the image.

Advection term: $S_t = -\langle \nabla_g, \vec{n} \rangle \vec{n}$ with associated level set equation $\phi_t = \nabla_g \cdot \nabla_\phi$.

The advection term produces an alignment of the normal vector to the surface with the gradient of the image. In places of high gradient, this term acts like a potential valley that forces the surface to stop the evolution at the strongest local minimum of that valley. This phenomenon is illustrated in Figure 1.

In summary, when the surface evolves in flat gradient places, the region based term leads the evolution smoothed by the curvature based term. When the surface reaches the potential valley generated by the strongest edges in the image, $k_{out} - k_{in} \approx 0$, because in transition places the inner and the outer PDF are similar and the curvature term is almost zero. So, only the advection term drives the evolution of the surface producing an attraction to the boundaries of the object.

(A4) Considering the functional

$$E_{GAC}(S(t)) = \int \int g(S(t))da, \tag{10}$$

as the surface evolves towards the edges of the image $E_{GAC}(S(t))$ decreases. At the steady-state, $E_{GAC}(S(t+1)) - E_{GAC}(S(t)) \approx 0$. Computing

this quantity and check in each iteration if it is less than a threshold can be a possible convergence criterion.

(A5) In the performance of manual measurements using MIP images, the observer subjectivity can be introduced from two ways. The first one, is the selection of the window levelling, that is used to enhance the structures of interest in low contrast images. This may cause an apparent change of the dimensions of the aneurysms. The second one, is the selection of the optimal angle. In some images, overlapping structures may cause a misinterpretation of the image leading to wrong measurements.

Using the 3D model, the boundaries of the model match exactly with the true edges of the aneurysms. There are more possibilities in the selection of the optimal viewpoint than in MIP images. There is no possibility of a misinterpretation of the image due to overlapping structures since the model can be interactively rotated in any position.

The evaluation study presented in this chapter aims to demonstrate that the same accuracy can be obtained with the 3D models than with the manual method. For this purpose, measurements from the 3D models were done emulating MIP-based ones and compared with the manual ones using the Bland-Altman plots. To take real advantage from the potentiality of the 3D models, automatic algorithms for the extraction of the 3D measurements should be designed. In fact, this is part of our future work.